American Mineralogist, Volume 79, pages 240–249, 1994

OH incorporation in synthetic clinopyroxene

HENRIK SKOGBY*
Institute of Earth Sciences, Mineralogy-Petrology, Uppsala University, Norbyvägen 18B, S-752 36 Uppsala, Sweden

ABSTRACT

A series of pyroxene crystals of diopside composition, doped with different cations, was synthesized to study OH incorporation in the pyroxene structure. Flux-growth methods were applied to obtain single crystals suitable for infrared spectroscopy. Samples were grown both in air and under controlled f_{H_2}/f_{O_2} using a H_2-CO_2 gas mixing furnace. Heating of samples containing Fe^{3+} in a H_2 atmosphere at 700 or 800 °C proved to be an efficient way to incorporate OH in the pyroxene structure. The IR spectra of these hydrous synthetic pyroxene crystals are similar to those of natural diopside, without reduction of the spectral complexity. Concentrations of up to 1100 ppm H_2O, compatible with the most hydrous pyroxene samples known, could be obtained. H was to a large extent taken up according to the reduction-hydrogenation reaction $Me^{3+} + O^{2-} + \frac{1}{2}H_2 = Me^{2+} + OH^-$, where Me is either Fe or Mn. The changes in oxidation state of Fe and Mn could be followed by Mössbauer spectroscopy and optical absorption spectroscopy.

The samples grown in the H_2-CO_2 gas mixing furnace took up OH in relation to the gas mixing ratio. However, considerably smaller amounts were taken up by the samples grown in the gas mix than by the Fe^{3+}-rich samples grown in air that were heated in H_2.

The results demonstrate that large amounts of OH can be taken up by clinopyroxene after crystallization under certain conditions, and that the kinetics of the hydrogenation reaction need to be better investigated if OH incorporation in pyroxene is to be used as an indicator of the activity of hydrous components during their crystallization.

INTRODUCTION

Natural pyroxene commonly contains structurally bound OH. Its concentration varies widely, with reported values ranging from 5 to 1100 ppm H_2O (e.g., Ingrin et al., 1989; Skogby et al., 1990; Smyth et al., 1991; Bell and Rossman, 1992). The concentration correlates with geological environment, which implies that the OH incorporation may be related to the activity of hydrous components during crystallization, and that this OH content is afterward more or less preserved. In this way, the strong variation in OH concentration in pyroxene may reflect strong variations in the activity of hydrous components during crystal growth. Alternatively, OH may be related to other components (e.g., Na, $^{[4]}Al$) with H^+ acting as a charge compensator that enters the structure in the amount required by stoichiometry, but unrelated to H_2O activity.

The most hydrous pyroxene samples found are of mantle origin (Smyth et al., 1991), and pyroxene seems to be the most hydrous major mantle mineral. The capability of hydrous pyroxene to act as a repository for H_2O in the mantle, and also to recirculate H_2O from the crust to deep parts of the mantle, has been discussed by Bell and Rossman (1992).

Even though hydrous pyroxene seems to be significant in geological processes, the mechanisms controlling OH incorporation in pyroxene are poorly understood. They seem to depend both on internal factors such as the type of pyroxene and its chemical composition, and on external factors such as temperature, f_{O_2} and f_{H_2}, and H_2O activity prevailing during crystallization. The OH in pyroxene is relatively strongly bound, with a thermal stability similar to that of OH in the amphibole structure (Skogby and Rossman, 1989). Still, it is possible to dehydrate hydrous pyroxene experimentally by heat treatment in air and also to increase the amount of OH in some Fe^{3+}-rich samples by heat treatment in H_2.

The exact locations of the OH ions in the pyroxene structure are not precisely known. In *C2/c* pyroxene, H probably bonds to O in one of the normal O positions, forming an OH ion. A favorable position is the underbonded O2 position, which has bonds to one M1, one M2, and one tetrahedral position (Beran, 1976). The occurrence of OH on this position has been recently reported from XRD refinement studies on omphacite (Smyth et al., 1992). Among the nominally hydrous silicates, OH ions almost never bond directly to Si, and such Si avoidance behavior of OH can also be expected in clinopyroxene (Rossman and Smyth, 1990). Hence, substitution of trivalent ions for Si in the tetrahedral position bonded to O2 (thereby making O2 even more underbonded) may be essential for OH incorporation in cli-

* Present address: Swedish Museum of Natural History, Department of Mineralogy, Box 50007, S-104 05 Stockholm, Sweden.

0003–004X/94/0304–0240$02.00

nopyroxene. The capability of diopside, containing Fe^{3+} in the tetrahedral position, to accommodate large amounts of OH has been experimentally demonstrated (Skogby and Rossman, 1989). There might be, however, more than one position that can accommodate OH in the clinopyroxene structure. Infrared spectroscopy, the commonly used technique to detect OH, yields rather complex spectra composed of several bands with different polarization, implying that several local environments for the OH ion are present in the pyroxene structure. One of the OH bands in the spectra of clinopyroxene has been demonstrated to be correlated with M2-site vacancies (Smyth et al., 1991). Other bands also show some correlation with chemical composition (Skogby et al., 1990), but the problem of the spectral complexity in general has not been solved. Neither are the maximum levels of OH incorporation in pyroxene known.

The aim of this work was to study how the OH absorptions in the infrared spectrum of hydrous clinopyroxene are related to the sample composition by use of synthetic pyroxene of controlled chemistry and to study how different crystallization environments, in terms of f_{O_2} and f_{H_2}, affect the amount of OH incorporated during crystal growth.

Experimental procedure

Synthesis

Fourier-transform infrared absorption spectroscopy (FTIR) is commonly used to study OH ions in pyroxene. Information on the amount of OH and the orientation of the OH dipole can be obtained from the polarized spectra of oriented single crystals. These spectra require crystals with a smallest dimension of around 100 μm and, for low OH concentrations, several hundred micrometers. Because such a crystal size is difficult to obtain by conventional hydrothermal synthesis techniques, flux-growth methods were used in this study. A successful method involved slow cooling of a homogenized melt of the pyroxene components (nutrient) and $Na_2B_4O_7$ (flux). The experiments were conducted at 1 atm in air and also under controlled atmosphere in a gas mixing furnace. The use of $Na_2B_4O_7$ as a flux was favored because it is stable under reducing conditions, which is usually not the case for other flux compounds, such as vanadates, used for pyroxene growth (Carlson, 1986a, 1986b). Starting mixtures were prepared by grinding oxides mixtures for the desired pyroxene composition with some excess silica and the $Na_2B_4O_7$ flux. A nutrient to flux ratio of 2:1 to 2.5:1 by weight was used. Melting test experiments showed these mixtures to form homogenous melts around 1100 °C. Quantities of 3–6 g of the mixtures were put into Pt crucibles, covered by a lid, placed in a furnace, and brought up to 1100 or 1200 °C. The charges were held at these temperatures for 24 h to homogenize, before onset of a slow cooling (2 or 4 °C per hour) to 700–900 °C.

In order to control the f_{O_2} during crystal growth, some experiments were performed in a H_2-CO_2 gas mixing furnace. The experimental setup consisted of a vertical tube furnace where the Pt crucible was suspended from the top. The H_2 and CO_2 gases were controlled by mass flow regulators and mixed before entering the furnace at the bottom. Three gas mixes corresponding approximately to the FeO-Fe_3O_4 and Fe-FeO solid buffers and to 1.2 log units in f_{O_2} below the Fe-FeO buffer were applied. The gas mix ratios were kept uniform during each experiment, resulting in a decrease of the f_{O_2} during the cooling stage of the experiment, similar to the behavior of solid buffers on cooling (cf. Huebner, 1987).

Table 1. Starting compositions and experimental conditions for flux-grown clinopyroxene

Expt.	Starting composition*	Nutrient : flux (g)	Atmosphere	T (°C)	Cooling rate (°C/h)
Samples grown in air					
Di-2	$Ca_{1.0}Fe_{0.2}Mg_{0.8}Si_2O_6$	2:1	air	1100–700	2
Di-3	$Ca_{1.0}Fe_{0.1}Mg_{0.8}Al_{0.1}Si_2O_6$	2:1	air	1100–700	2
Di-5	$Ca_{1.0}Fe_{0.5}Mg_{0.5}Si_2O_6$	4:2	air	1100–700	2
Di-6	$Ca_{1.0}Fe_{0.1}Mg_{0.7}Cr_{0.1}Al_{0.1}Si_2O_6$	4:2	air	1100–700	2
Di-12	$Ca_{1.0}Fe_{0.2}Mg_{0.7}Al_{0.2}Si_{1.9}O_6$	4:1.6	air	1200–800	2
Di-13	$Ca_{1.0}Fe_{0.1}Mg_{0.8}Cr_{0.1}Si_2O_6$	4:1.6	air	1200–800	2
Di-15	$Ca_{1.0}Fe_{0.04}Mg_{0.96}Si_2O_6$	4:1.6	air	1200–800	4
Di-16	$Ca_{1.0}Mn_{0.2}Mg_{0.8}Si_2O_6$	4:1.6	air	1200–800	4
Samples grown in gas mix			$H_2 : CO_2$**		
Di-7	$Ca_{1.0}Fe_{0.5}Mg_{0.5}Si_2O_6$	4:2	1:1	1100–700	2
Di-14	$Ca_{1.0}Fe_{0.5}Mg_{0.5}Si_2O_6$	4:1.6	1:10	1200–900	2
Di-17	$Ca_{1.0}Fe_{0.5}Mg_{0.5}Si_2O_6$	4:1.6	5:1	1200–900	2

Note: the flux consisted of $Na_2B_4O_7$. The experiments were equilibrated at the starting temperature for 24 h before the cooling stage began.

* An excess of 30% silica was added to the starting composition.

** Gas volume mixing ratio. Total flow was regulated to 60–90 mL/min (cold gases).

Mostly diopside, doped with a single or several foreign elements, was grown. For samples grown in air, a reducible element (Fe^{3+} or Mn^{3+}) was added. Details of the different experiments are given in Table 1.

Experimental products consisted of clinopyroxene crystals, precipitating mostly from the wall and bottom of the crucible but also from the surface of the melt. The sodium borate glass was dissolved first in hot diluted HCl and then in a cold NaOH solution, a procedure that required a few days but was shortened by the use of an ultrasonic bath. Most experiments yielded 0.5–1 g of clinopyroxene crystals of variable size, the largest around 1 × 1 × 5 mm. The crystals are elongated along the **c** axis and usually have well-developed (110) surfaces and sometimes also smaller (100) and (010) surfaces. The larger crystals frequently have cracks and often contain conical hollow ends (hourglass texture).

To incorporate H in the samples, selected crystals were afterward heat treated in pure H_2 gas (at 1 atm) at 700 or 800 °C, using a horizontal tube furnace. The temperature and duration of this treatment were chosen according to experiments on natural diopside (Skogby and Rossman, 1989), which showed that OH bands in the IR spectra removed by heating millimeter-sized samples in air are restored after heating in H_2 at 600–700 °C for 6 h. How-

Table 2. Electron microprobe analyses (wt%) and structural formulae for synthetic clinopyroxene

Sample	Di-2	Di-3	Di-5	Di-6	Di-7	Di-12	Di-13	Di-14	Di-15	Di-16	Di-17
SiO_2	54.44	54.62	50.69	53.75	51.58	54.29	52.75	52.84	54.75	53.89	54.24
Al_2O_3	—	0.16	—	0.20	—	0.24	—	—	—	—	—
Cr_2O_3	—	—	—	1.76	—	—	2.07	—	—	—	—
Fe_2O_3	3.56	2.00	12.50	2.91	1.03	3.21	1.49	0.82	0.80	—	0.15
FeO	0.19	0.14	—	0.18	11.30	0.38	0.19	5.99	—	—	4.22
Mn_2O_3	—	—	—	—	—	—	—	—	—	2.57	—
MgO	16.90	17.73	12.17	15.71	10.84	16.64	16.41	14.47	18.68	17.37	16.01
CaO	23.66	24.59	20.12	23.38	23.77	23.95	23.57	24.20	24.98	24.80	25.00
Na_2O	0.91	0.61	2.70	1.34	0.36	0.93	1.07	0.31	0.25	0.15	0.16
Total	99.66	99.85	98.18	99.23	98.88	99.64	97.55	98.63	99.46	98.78	99.78
Tetrahedral positions											
Si	1.986	1.983	1.927	1.977	1.987	1.982	1.971	1.989	1.988	1.980	1.997
Al	—	0.007	—	0.009	—	0.008	—	—	—	—	—
Fe^{3+}	0.014	0.005	0.032	0.010	—	0.010	0.006	—	—	—	—
Octahedral positions											
Al	—	—	—	—	—	0.002	—	—	—	—	—
Cr	—	—	—	0.051	—	—	0.061	—	—	—	—
Fe^{3+}	0.084	0.050	0.326	0.071	0.030	0.079	0.036	0.023	0.022	—	0.004
Fe^{2+}	0.006	0.004	—	0.006	0.364	0.012	0.006	0.189	—	—	0.130
Mn^{3+}	—	—	—	—	—	—	—	—	—	0.072	—
Mg	0.919	0.960	0.690	0.861	0.623	0.906	0.914	0.812	1.011	0.951	0.879
Ca	0.925	0.957	0.820	0.921	0.981	0.937	0.944	0.976	0.972	0.976	0.986
Na	0.064	0.043	0.199	0.096	0.027	0.066	0.078	0.023	0.018	0.011	0.011
Total	3.998	4.009	3.994	4.002	4.012	4.001	4.016	4.012	4.011	3.990	4.007

Note: the structural formulae were normalized to six O atoms. The distribution and oxidation state of Fe was determined by Mössbauer spectroscopy (except Di-15). Minor B contents (up to 0.6 wt% B_2O_3) are assumed to be present in the samples (cf. Hålenius and Skogby, unpublished manuscript).

ever, the OH concentrations reported here are not considered to represent equilibrium values. The heating experiments on natural diopside showed that the IR band intensities actually decrease during prolonged heating periods in H_2.

Analysis

Chemical analyses on the crystals were performed with a Cameca SX50 electron microprobe, using a sample current of 15 nA and an accelerating potential of 20 kV. The crystals usually are zoned, in the case of Fe-bearing samples with an Fe-poor and Mg-rich core and an Fe-rich and Mg-poor edge. The zonation studies show that Fe is enriched in the melt during crystal growth, which is also evident from the analysis, since the crystals always contain less Fe than the starting composition. Because of this compositional heterogeneity of the crystals, the analyzed spots were selected in the same areas as were used for the IR spectroscopy. The results from the microprobe analyses and the structural formulae of the samples, normalized to six O atoms, are given in Table 2. According to the pyroxene nomenclature (Morimoto et al., 1988), most of the samples are diopside with various amounts of an aegirine component, but one sample (Di-5) falls in the aegirine augite compositional field. Only minor amounts of Al were taken up by Al-doped samples. Since the crystals were grown in a B-containing melt, they are expected to incorporate B to some extent. B was not analyzed in the present study but has been analyzed by secondary ion mass spectroscopy (SIMS) for a number of Mn-containing diopside samples grown under the same conditions (Hålenius and Skogby, unpublished manuscript), giving B_2O_3 contents of 0.18–0.51 wt%. Similar B contents are assumed to be present in the samples studied here. The small trivalent B ion probably substitutes for Si (around 0.01–0.03 B pfu), thereby increasing the somewhat low sums of tetrahedral ions in the normalized formulae.

Sample preparation for FTIR spectroscopy was done by orienting crystals using their morphology and optical extinction. The samples were then ground and doubly polished to obtain a clear viewing path of appropriate size. Sections were usually prepared on (100) and (010) surfaces and occasionally on well-developed (110) growth surfaces. Polarized infrared spectra were obtained in the three principal vibration directions (α, β, and γ) for most of the samples, using a Nicolet 60SX Fourier-transform IR spectrophotometer equipped with a $LiIO_3$ Glan polarizer. The self-supporting sample sections, with thicknesses measuring usually from 100 to 300 μm, were placed on stainless steel apertures with diameters of 200–600 μm. The amount of OH in the samples was calculated as H_2O concentration, according to the Beer-Lambert law, giving H_2O_{conc} = absorbance/(ϵ_{H_2O}·path length) where ϵ_{H_2O} is the molar absorptivity of H_2O. The absorbance was calculated as the summed absorbance (peak height intensity) of all individual peaks in the three principal vibration directions (cf. Skogby et al., 1990). The base line was estimated visually. Molar absorptivities of OH in pyroxene have been determined by calibrations with a number of independent methods (Wilkins and Sabine, 1973; Skogby et al., 1990), most of which converge toward a mean value around 150 $mol^{-1}L^{-1}$ for OH (and twice of that if H_2O is considered). A recent calibration obtained on diopside (Bell et al., unpublished manuscript), gave ϵ_{H_2O} = 316 $mol^{-1}L^{-1}$ (= ϵ_{OH} = 158 $mol^{-1}L^{-1}$), which was used to calculate the OH concentrations (in ppm H_2O) in the present studied synthetic samples. Sample densities needed to calculate the OH concentration

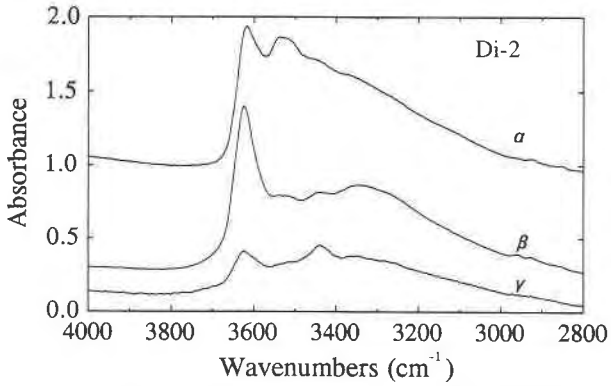

Fig. 1. Infrared absorption spectra of Fe^{3+}-doped diopside (Di-2), heated in H_2 at 800 °C, in the α, β, and γ polarization directions. The spectra are normalized to a 1-mm sample thickness and vertically offset for clarity.

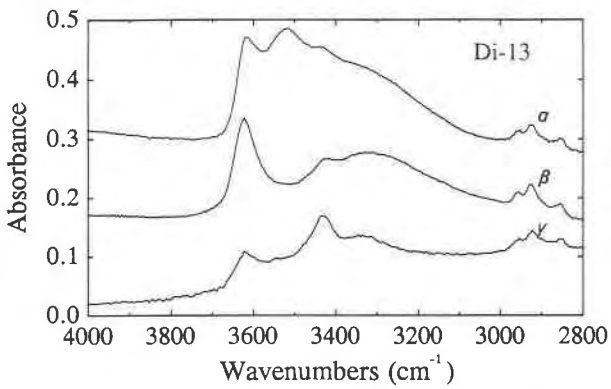

Fig. 3. Polarized IR spectra of synthetic Cr- and Fe^{3+}-doped diopside (Di-13), heated in H_2 at 800 °C, normalized to a 1-mm thickness. Weak absorptions around 2900 cm^{-1} are due to organic contaminants.

were estimated from their chemical composition using data in Deer et al. (1966). For a few samples for which only unpolarized spectra were obtained, the OH concentration was estimated by comparison with unpolarized spectra of samples of known OH concentration.

Determination of the oxidation state of Fe in the samples was made by Mössbauer spectroscopy. The procedure of data collection was similar to that described in Skogby et al. (1992), using a source of ^{57}Co in Rh matrix and a 512 channel multichannel analyzer. Samples were held at room temperature and at an angle of 54.7° to the incident γ beam to avoid orientation effects. Spectrometer velocity was calibrated against Fe foil. The spectra were fitted by least-squares methods using Lorentzian peak shapes with one doublet each for $^{[6]}Fe^{2+}$, $^{[6]}Fe^{3+}$, and $^{[4]}Fe^{3+}$ and a peak assignment similar to that given by Akasaka (1983) and Dollase and Gustafson (1982). The area ratios of the fitted doublets were used to calculate the Fe distribution.

For a Mn-doped sample (Di-16), the occurrence of Mn^{3+} before and after H_2 treatment was studied by optical spectroscopy in the visible range, using a prototype fiber optics spectrometer equipped with a diode array detector.

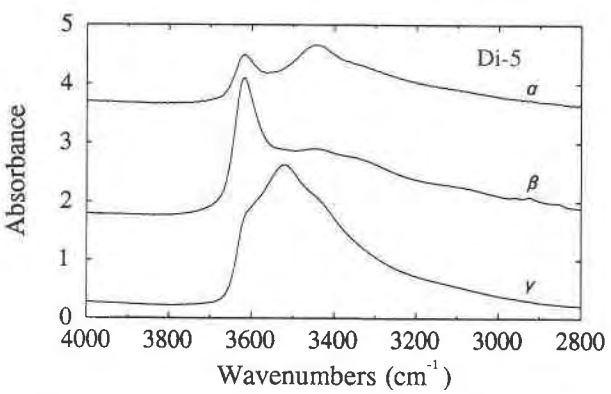

Fig. 2. Polarized IR spectra of aegirine augite (Di-5), heated in H_2 at 700 °C, normalized to a 1-mm thickness.

Results

Air-grown samples

Before heat treatment in H_2, the IR spectra of clinopyroxene grown in air do not show any absorption features in the OH region. After the H_2 treatment, bands appear in the spectra of all air-grown samples, which all contain a reducible species (i.e., Fe^{3+} or Mn^{3+}). Representative spectra of the H_2-heated samples polarized in the α, β, and γ directions are shown in Figures 1–4. The IR spectra of these synthetic samples are similar to those obtained on natural samples, usually dominated by a band around 3620 cm^{-1}, strongest in the α and β directions, and another band around 3520 cm^{-1}, strongest in the γ direction. Most spectra also have weaker bands at other positions. A summary of band positions and their absorbances is given in Table 3. The band widths are similar to or slightly larger than the bands obtained on natural samples. The calculated OH concentrations, given in Table 3, range from 3 ppm H_2O (Di-15) to 1100 ppm H_2O (Di-5), and there is a clear trend of increasing OH

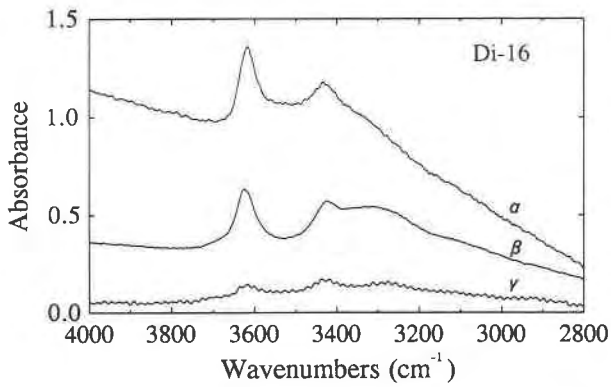

Fig. 4. Polarized IR spectra of synthetic Mn-doped diopside (Di-16), heated in H_2 at 800 °C, normalized to a 1-mm thickness. The weak high-frequency sinusoidal modulations are due to interference fringes, not sample absorbance.

Table 3. Intensity of OH bands in the infrared spectrum and calculated OH concentrations for synthetic clinopyroxene

Sample	H_2 treatment T (°C)	Linear absorbance (mm^{-1}) Wavenumber (cm^{-1}) 3620–3640	3520–3535	3440–3450	3350–3360	3300	Σ_{abs} (mm^{-1})	OH conc. (ppm H_2O)	(OH pfu)
Samples grown in air*									
Di-2	800	2.08	0.26	0.44	0.26	—	3.04	500	0.012
Di-3	700	0.51	0.03	—	—	0.24	0.78	125	0.003
Di-5	700	3.25	2.14	1.56	—	—	6.95	1100	0.028
Di-6	700	1.23	0.66	—	0.49	—	2.38	390	0.009
Di-12	800	1.76	0.26	0.50	0.38	—	2.90	480	0.012
Di-13	800	0.36	0.08	0.16	—	—	0.60	100	0.002
Di-15	800	0.02	—	—	—	—	0.02	3	0.0001
DI-16	800	0.72	—	0.41	—	—	1.13	190	0.005
Samples grown in gas mix**									
Di-7	untr.	0.035	0.020	—	0.016	—	0.071	26	0.0007
Di-7	700	0.069	0.019	—	0.031	—	0.119	45	0.0011
Di-14	untr.	0.004	0.008	—	0.004	—	0.016	6	0.0002
Di-14	700	0.069	0.019	—	0.031	—	0.119	45	0.0011
Di-17	untr.	0.023	0.012	—	0.020	—	0.055	21	0.0005

Note: the OH concentration was calculated using $\epsilon_{H_2O} = 316$ mol^{-1}L^{-1}.

* The given absorbance values represent summed absorbances in the α, β, and γ directions for the individual bands.

** The given absorbance values are obtained from unpolarized spectra on (110) sections; OH concentration determined by comparison with corresponding spectra of samples of known OH concentration.

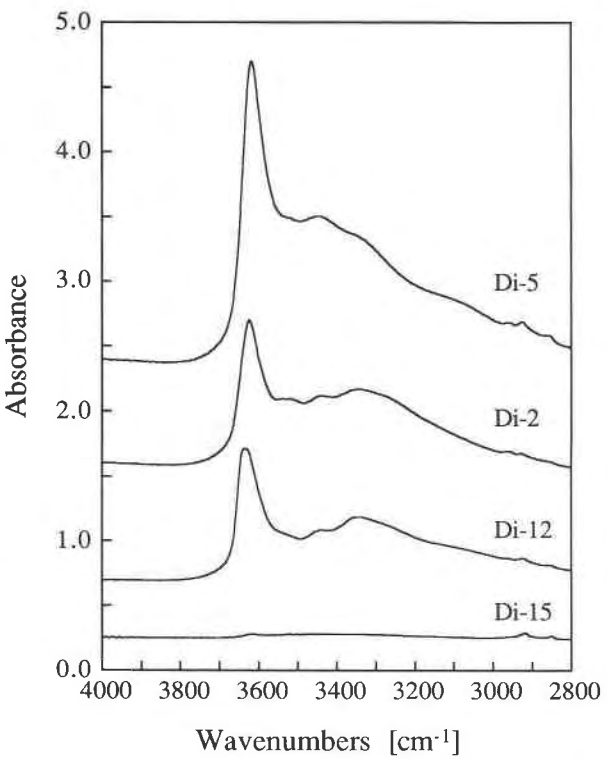

Fig. 5. IR spectra of diopsidic pyroxene containing various amounts of Fe normalized to a 1-mm thickness. From top to bottom: Di-5: $Fe_{tot} = 0.36$ pfu, heated in H_2 at 700 °C, β polarization on (100) section. Di-2: $Fe_{tot} = 0.10$ pfu, heated in H_2 at 800 °C, β polarization on (100) section. Di-12: $Fe_{tot} = 0.10$ pfu, heated in H_2 at 800 °C, β polarization on (100) section. Di-15: $Fe_{tot} = 0.02$ pfu, heated in H_2 at 800 °C, unpolarized spectrum on (010) section.

concentration for increasing Fe^{3+} concentration, as can be seen in Figure 5. The most hydrous sample has an H_2O content similar to that of the most hydrous pyroxene samples reported (cf. Smyth et al., 1991).

The Mössbauer spectra obtained on the air-grown samples show that Fe generally occurs as Fe^{3+} (Table 4). Most of the Fe^{3+} is present in the octahedral positions, but all air-grown samples containing Fe also have some $^{[4]}Fe^{3+}$. In most cases, minor amounts of Fe^{2+} are present. Heat treatment in pure H_2 gas reduces some Fe^{3+} to Fe^{2+} (Fig. 6), but all samples still contain Fe^{3+} after the H_2 heat treatment. Mainly Fe^{3+} in the octahedral position is reduced, as changes in the rather weak peak due to Fe^{3+} in the tetrahedral position are not significant.

Samples grown in gas mix

The clinopyroxene crystals that were grown under reducing conditions in the gas mixing furnace all show absorption bands in the OH region of their IR spectra (cf. Figs. 7, 8). Two of these samples were grown under identical conditions, apart from different H_2-CO_2 gas mixing ratios. Sample Di-14, which was grown at a relatively high f_{O_2} (H_2:CO_2 = 1:10; corresponding approximately to the FeO-Fe_3O_4 solid buffer), contains 6 ppm H_2O, whereas Di-17, grown at a low f_{O_2} (H_2:CO_2 = 5:1; approximately 1.2 log f_{O_2} units below the Fe-FeO solid buffer), contains 21 ppm H_2O. The third sample (Di-7), which was grown with a larger flux component at moderate f_{O_2} (H_2:CO_2 = 1:1; Fe-FeO buffer), contains 26 ppm H_2O. This comparatively high concentration may be due to a decrease in f_{O_2} caused by a lower precipitating temperature, in turn caused by the larger flux to nutrient ratio. The sample also has a significantly higher Fe content than

TABLE 4. Fe distribution before and after heat treatment in H_2

Sample	H_2 treatment T (°C)	Fe distribution			Atoms per formula unit		
		$^{[6]}Fe^{2+}$	$^{[6]}Fe^{3+}$	$^{[4]}Fe^{3+}$	$^{[6]}Fe^{2+}$	$^{[6]}Fe^{3+}$	$^{[4]}Fe^{3+}$
Samples grown in air							
Di-2	untr.	0.055	0.806	0.139	0.006	0.084	0.014
Di-2	800	0.267	0.672	0.061	0.028	0.070	0.006
Di-3	untr.	0.070	0.846	0.084	0.004	0.050	0.005
Di-3	700	0.402	0.480	0.118	0.024	0.028	0.007
Di-5	untr.	nd	0.912	0.088	—	0.326	0.032
Di-5	700	0.139	0.800	0.061	0.050	0.286	0.022
Di-6	untr.	0.064	0.821	0.115	0.006	0.071	0.010
Di-6	700	0.323	0.580	0.098	0.028	0.050	0.009
Di-12	untr.	0.115	0.789	0.096	0.012	0.079	0.010
Di-12	800	0.288	0.606	0.106	0.029	0.061	0.011
Di-13	untr.	0.122	0.758	0.120	0.006	0.036	0.006
Di-13	800	0.354	0.524	0.122	0.017	0.025	0.006
Samples grown in gas mix							
Di-7	untr.	0.926	0.074	nd	0.364	0.030	—
Di-7	700	0.926	0.074	nd	0.364	0.030	—
Di-14	untr.	0.890	0.110	nd	0.189	0.023	—
Di-14	700	0.896	0.104	nd	0.190	0.022	—
Di-17	untr.	0.969	0.031	nd	0.130	0.004	—
Di-17	700	0.982	0.018	nd	0.132	0.002	—

Note: the Fe distribution is obtained from the area ratios of the fitted doublets in the Mössbauer spectra; nd = not detected.

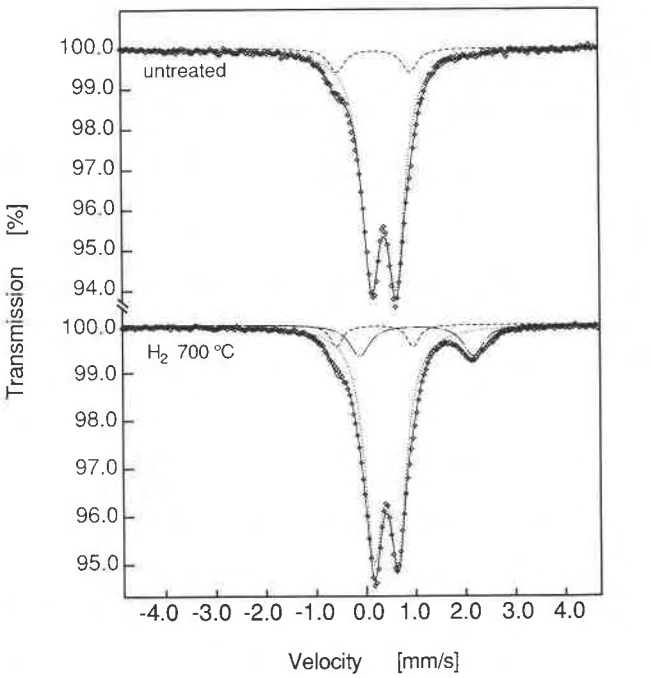

Fig. 6. Mössbauer spectra of aegirine augite (Di-5) before and after heat treatment in H_2 at 700 °C for 6 h. Note the appearance of an Fe^{2+} doublet in the spectrum of the H_2-treated sample. Dotted doublet: $^{[6]}Fe^{3+}$; dashed doublet: $^{[4]}Fe^{3+}$; dashed and dotted doublet: $^{[6]}Fe^{2+}$.

the other two samples grown in the gas mix (Table 2), even though the starting nutrient compositions were the same.

The OH content increased also for the samples grown in the gas mix when they were heated in pure H_2 gas. The OH increase is highest for the sample grown at the lowest H_2/CO_2 ratio (Di-14; Fig. 8), which also had the highest Fe^{3+}/Fe_{tot} ratio before heat treatment. After the heat treatment in H_2, samples Di-7 and Di-14 both reach the same OH content, corresponding to 45 ppm H_2O (Table 3).

Mössbauer spectra of samples grown in the gas mixing furnace show that Fe mostly occurs as Fe^{2+} (Fig. 9). These samples also contain some Fe^{3+}, which gradually increases from $Fe^{3+}/Fe_{tot} = 0.03$ in the sample grown in the most reducing atmosphere to $Fe^{3+}/Fe_{tot} = 0.11$ in the sample grown in the least reducing atmosphere (Table 4). Only minor changes in the Fe^{3+}/Fe_{tot} ratio were observed after the H_2 heat treatment. The small amounts of Fe^{3+} are probably stabilized as an aegirine component as a result of the Na-rich melt. The samples have Na contents similar to the Fe^{3+} contents, which can be expressed as a 1–3% aegirine ($NaFe^{3+}Si_2O_6$) component.

Color changes usually follow heat treatment in H_2. The color of Fe-containing samples grown in air ranges from yellow to brown as the Fe content increases. This color is most probably caused by $^{[4]}Fe^{3+}$ (Bell and Mao, 1972). When these samples are heat treated in H_2, the color changes toward dark green or brownish green, probably because of Fe^{2+}-Fe^{3+} charge-transfer absorption, which can take place as some of the Fe^{3+} is reduced to Fe^{2+}. The Mn-containing sample (Di-16) grown in air is violet. The optical spectrum of this sample contains absorption peak near 530 nm (Fig. 10), which is assigned to Mn^{3+}. Absorption bands in this region in the spectra of natural pyroxene containing Mn^{3+} have been assigned to spin-allowed d-d transitions in Mn^{3+} in the M1 position (cf. Ghose et al., 1986). After heat treatment of the samples in H_2, the peak decreased in intensity and even disappeared in small grains.

DISCUSSION

The spectra obtained on H_2-heated pyroxene grown in air and doped with various cations are rather similar in terms of band position and polarization, as can be seen in Figures 1–5. There is no clear correlation of band position and chemical composition, and, hence, it is not possible to assign specific bands to specific cation arrangements close to the absorbing OH dipole. For amphiboles, cation substitutions close to the OH position have been demonstrated to cause shifts in the band positions of about 6–15 cm^{-1} (Burns and Strens, 1966; Skogby and Rossman, 1991). Any major band shift cannot be observed for the synthetic pyroxene samples, but since the pyroxene bands are significantly broader than those of amphiboles, peak shifts smaller than 10 cm^{-1} may be difficult to discern. The relatively narrow pyroxene band around 3620 cm^{-1} actually shifts around 10 cm^{-1} between the Al-doped Di-12 and the Al-free Di-2

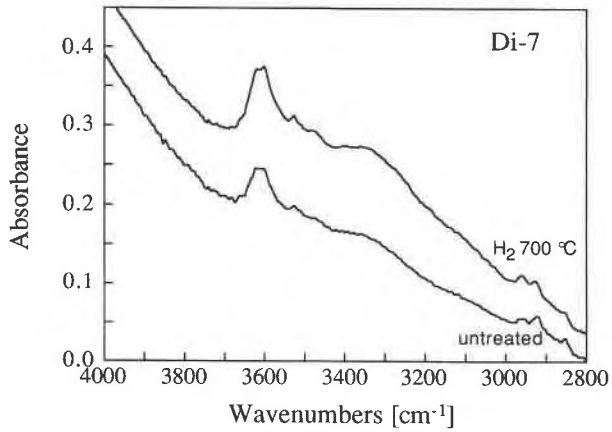

Fig. 7. IR spectra of diopside grown under H_2-CO_2 gas with a mixing ratio of 1:1 (approximately corresponding to the Fe-FeO solid buffer), before and after heat treatment in pure H_2 at 700 °C for 6 h. The unpolarized spectra are normalized to a 1-mm thickness and were obtained on (110) sections.

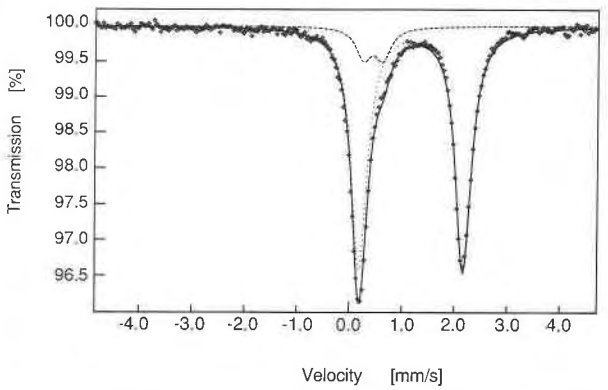

Fig. 9. Mössbauer spectrum of diopside (Di-14), grown in a gas mixing furnace with a H_2:CO_2 ratio of 1:10. Dashed doublet: $^{[6]}Fe^{3+}$; dotted doublet: $^{[6]}Fe^{2+}$.

and Di-5 (Fig. 5). A complicating factor may be the presence of Na and B in the synthetic samples, stemming from the $Na_2B_4O_7$ flux. If the OH incorporation is associated with substitution of trivalent ions for Si, as mentioned earlier, the somewhat broader bands obtained on the synthetic samples may be caused by substitution of both Fe^{3+} and B (and in some samples Al) on the tetrahedral site.

Nevertheless, some relations between chemical composition of a sample and the resulting spectrum can be observed. All Fe-containing samples have a band around 3530 cm^{-1} in their spectra, whereas the spectrum of the Mn-doped Fe-free sample (Di-16) does not have such a band (Fig. 4). This indicates that the 3530-cm^{-1} band is associated with Fe, an observation that has also been made for natural samples (Skogby et al., 1990).

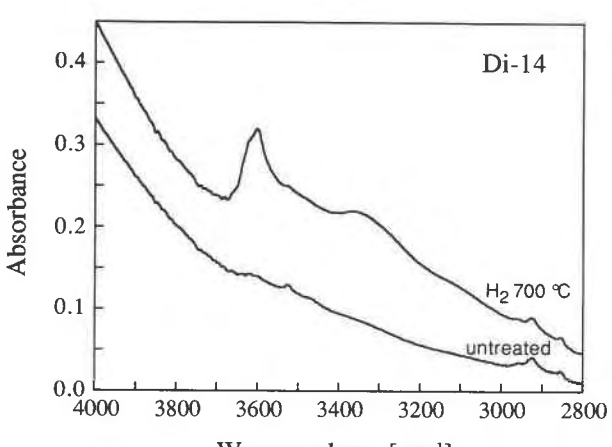

Fig. 8. IR spectra of diopside grown under H_2-CO_2 gas with a mixing ratio of 1:10 (approximately corresponding to the FeO-Fe_3O_4 solid buffer), before and after heat treatment in pure H_2 at 700 °C for 6 h. The unpolarized spectra are normalized to a 1-mm thickness and were obtained on (110) sections.

The samples grown in the gas mixing furnace at different H_2-CO_2 ratios are of interest in evaluating the control of growth environment on OH uptake. Only two of the gas mixing samples (Di-14 and Di-17) should be compared, since the third sample (Di-7) was grown with a different flux to nutrient ratio and at lower temperatures than the former samples. Even though the OH absorption bands in the spectra of these samples are rather weak (Figs. 7, 8), it is evident that considerably more OH is taken up by crystals growing at high f_{H_2}/f_{O_2} (Di-17; 21 ppm H_2O) than by crystals growing at low f_{H_2}/f_{O_2} (Di-14; 6 ppm H_2O). It is not clear why these samples, also after heat treatment in H_2, have substantially lower OH concentrations than the H_2-treated samples grown in air. However, it is possible that the OH incorporation is reduced by the low f_{H_2O} (<0.4 bar) in the experiments. H initially incorporated may also be lost at high temperatures during the long synthesis period, similar to what has been observed for natural pyroxene heated in H_2 (Skogby and Rossman, 1989).

Hydration processes

Experimental incorporation of H in Fe^{3+}-rich natural pyroxene by heating in H_2 atmosphere largely takes place with charge compensation according to the reduction-hydrogenation reaction $Fe^{3+} + O^{2-} + \frac{1}{2}H_2 = Fe^{2+} + OH^-$ (Skogby and Rossman, 1989). The reversed reaction (oxidation-dehydrogenation) could also be confirmed when natural samples were heated in air. The same reaction has been extensively studied for hydrous silicates, e.g., amphiboles (Clowe et al., 1988). For the synthetic pyroxene samples containing Fe^{3+}, the reduction-hydrogenation reaction could be traced by Mössbauer spectroscopy, which showed that the Fe^{2+} content had increased after heating in H_2 (Table 4). The amount of reduction is higher than the amount of accommodated OH (cf. Fig. 11).

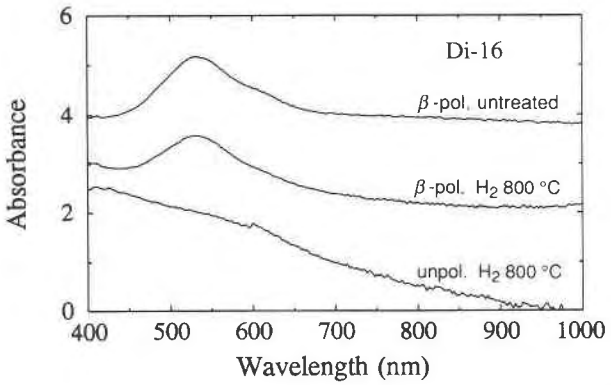

Fig. 10. Optical absorption spectra of Mn-doped diopside (Di-16), obtained before and after heat treatment in H_2. Spectra are normalized to a 1-mm thickness. Top: untreated sample; β-polarization on (100) section, the band at 530 nm is caused by Mn^{3+}. Middle: heat treated in H_2 at 800 °C for 6 h; β polarization on (100) section. Note the decrease of the 530-nm band. Bottom: unpolarized spectrum on (110) section of a small crystal (cleavage fragment) heated in H_2 at 800 °C for 6 h. Note disappearance of the 530-nm band.

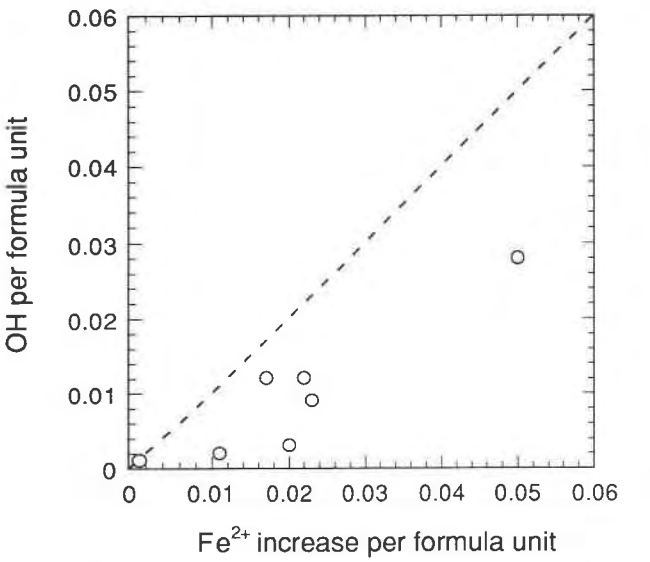

Fig. 11. Amount of OH incorporated in synthetic pyroxene during heat treatment in H_2, plotted vs. the amount of Fe^{2+} formed by the reduction of Fe^{3+}. The dashed line indicates the 1:1 relation.

This may be partly due to differences in the material studied by the two methods, since the IR study was made on the largest crystals possible, whereas the material used for Mössbauer spectroscopy included smaller crystals, which are likely to react faster with the H_2 atmosphere. On the other hand, the excess reduction observed may also be charge balanced by formation of O vacancies. In the IR spectra of natural pyroxene the reduction of OH band intensity upon heating in H_2 has been interpreted, in analogy with studies on micas, as condensation of two OH ions, leaving an O^{2-} and an O vacancy, with H_2O diffusing out of the crystal (Skogby and Rossman, 1989). A similar reaction can also be expected for synthetic pyroxene and may explain the Fe^{3+} reduction in excess of H incorporation.

There is a correlation of Fe^{3+} content and the amount of OH taken up during H_2 heat treatment (Figs. 5, 12). However, it is not possible to conclude that an Fe^{3+}-rich pyroxene is always able to accommodate more OH than a Fe^{3+}-poor pyroxene. The reduction-hydrogenation reaction is not hindered by lack of Fe^{3+}, since all samples still contain most of their original Fe^{3+} after the H_2 heat treatment (Table 4). The observed correlation of OH concentration and initial Fe^{3+} content may instead be due to kinetic reasons. H diffusion in olivine has been demonstrated (Mackwell and Kohlstedt, 1990) to occur by migration of H^+ ions coupled to a counterflux of electron holes (i.e., the excess charge on the Fe^{3+} ion), and this is probably the main H transport mechanism also in an Fe-containing pyroxene. Hence, the rate of the hydrogenation reaction should decrease if the Fe ions are dispersed as in an Fe-poor sample. Heating experiments on natural diopside (Skogby and Rossman, 1989) have also indicated that Fe-poor diopside is dehydrated and rehydrated more slowly than Fe-rich diopside. The pyroxene poorest in Fe in this study (Di-15), which has a Fe content of only 0.02 apfu, is also the sample slowest to accommodate OH. During H_2 treatment at 800 °C, this sample takes up only 3 ppm H_2O, corresponding to reduction of $<1\%$ of its initial Fe^{3+} content, in contrast to the other Fe-containing samples grown in air, which take up OH corresponding to a reduction of 5–13% of their initial Fe^{3+} content. It seems that the amount of OH incorpo-

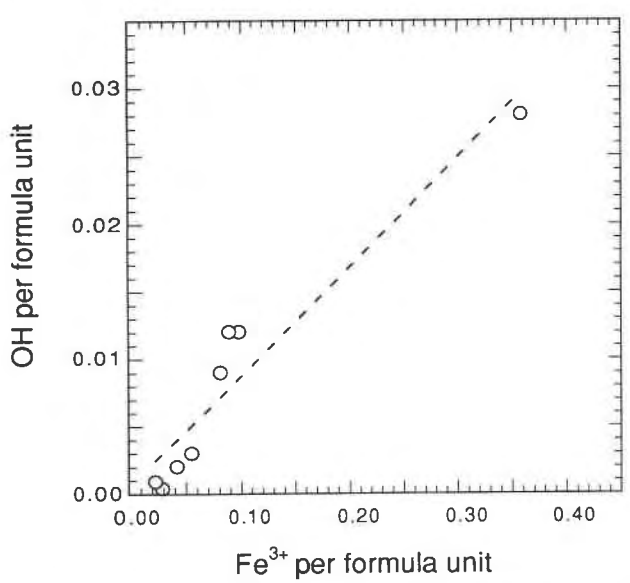

Fig. 12. Amount of OH incorporated in synthetic pyroxene during heat treatment in H_2, plotted vs. initial Fe^{3+} content. The dashed line represents a least-squares fit to the data.

rated during the H_2 heating experiments is a result of the combined effects of the concentration of suitable positions for the OH ion, the Fe^{3+} content (the driving force), and the Fe_{tot} content (the transport mechanism), where the first effect remains largely unknown but probably is influenced by tetrahedral substitutions. More experiments need to be performed to resolve these questions.

A reaction analogous to the Fe^{3+} reduction-hydrogenation reaction could be observed for the Mn^{3+} containing sample (Di-16), where the uptake of OH during H_2 heating was followed by a decreasing Mn^{3+} band in the visible region of the optical spectrum (Fig. 10). The Mn^{3+} reduction-hydrogenation reaction $Mn^{3+} + O^{2-} + \frac{1}{2}H_2 = Mn^{2+} + OH^-$ seems to be less efficient or slower than the Fe^{3+} reduction-hydrogenation reaction, as considerably less OH was taken up by the samples containing Mn^{3+} than by the corresponding samples containing Fe (cf. Di-2 and Di-16; Table 3). That Mn^{3+} was reduced to a higher degree in small grains than in large ones is probably due to kinetic effects.

Petrological implications

The results from the hydration experiments may provide some implications for the question of whether the OH recorded in pyroxene represents an initial incorporation at the time of crystallization, or if the OH may have reequilibrated to new conditions after crystallization. Bai and Kohlstedt (1992) suggested that the comparatively low OH contents detected in olivine from mantle xenoliths in basalt are due to H loss during the ascent stage, and that olivine within the mantle may contain concentrations of OH higher by a factor of ten. Similarly, the high Fe^{3+} and low H contents of hornblende megacrysts from basaltic flows have been interpreted (Dyar et al., 1992) to be due to partial dehydration during transportation from the mantle rather than high mantle f_{O_2} values. By contrast, pyroxene in basalt xenoliths are among the most hydrous pyroxene samples found and seem not to dehydrate during ascent.

For synthetic pyroxene, the observation that the air-grown (dry) samples during H_2 heating incorporate considerable amounts of OH, much more than the samples grown under reducing conditions, indicates that the growth environment may be of lesser importance than the post-crystalline conditions for the amount of OH accommodated in a natural sample. However, the heating experiments in pure H_2 represent extreme conditions in terms of f_{O_2}, which are not likely to be present in the crust or mantle. Pure H_2 provides a very strong driving force for Fe^{3+} reduction, which can only take place by H incorporation, unless O is removed from the structure (which is also expected in a long-term experiment). In the natural environment, postcrystallization uptake of H is expected to be less likely but could of course occur under some circumstances, e.g., if a pyroxene crystallized at relatively high f_{O_2} with considerable amounts of Fe^{3+} and was later exposed to more reducing and more hydrous conditions. From the H_2 heating experiments on pyroxene with varying amounts of Fe (Figs. 5, 12) it is clear that the Fe^{3+} reduction-hydrogenation reaction is accelerated by high Fe contents. Similarly, the reversed reaction (oxidation-dehydrogenation) should be accelerated by a high concentration of Fe or another multivalent element. This means that a pyroxene with a high concentration of multivalent elements will respond more readily to changes in f_{O_2}-f_{H_2} by changing its OH content than a pyroxene with low concentrations of such elements.

The results indicate that the amount of OH incorporated at crystallization is not a function of f_{O_2}-f_{H_2} only, since comparatively small amounts of OH were taken up by the samples grown in the gas mix, even at strongly reducing conditions, corresponding approximately to an f_{O_2} of 1.2 log units below the Fe-FeO buffer. P_{tot} and P_{H_2O} are also probably important. Preliminary results from hydrothermally grown orthopyroxene indicate that large amounts of OH are taken up during crystal growth at P_{H_2O} = 2.0 kbar and 800 °C.

The kinetics of the hydration and dehydration processes is a crucial issue when the OH content in natural pyroxene is used to estimate hydrous conditions prevailing at crystallization. The hydrogenation-dehydrogenation kinetics seems to be a function of at least Fe content, temperature, f_{O_2}, and f_{H_2}. In spite of that, the systematic correlation between OH concentration and geological environment (e.g., Skogby et al., 1990; Smyth et al., 1991; Bell and Rossman, 1992) indicates that the original OH concentrations are to a large extent preserved. However, there is a need to better investigate the kinetics of the reduction-hydrogenation reaction.

Acknowledgments

I am grateful to G.R. Rossman (Caltech) for discussions and comments and to J. Lindgren (Uppsala University) and G.R.R. for making their FTIR spectrometers available for this study. Financial support was given by the Swedish Natural Science Research Council.

References cited

Akasaka, M. (1983) ^{57}Fe Mössbauer study of clinopyroxenes in the join $CaFe^{3+}AlSiO_6$-$CaTiAl_2O_6$. Physics and Chemistry of Minerals, 9, 205–211.

Bai, Q., and Kohlstedt, D.L. (1992) Substitutional hydrogen solubility in olivine and implications for water storage in the mantle. Nature, 357, 672–674.

Bell, D.R., and Rossman, G.R. (1992) Water in earth's mantle: The role of nominally anhydrous minerals. Science, 255, 1391–1397.

Bell, P.M., and Mao, H.K. (1972) Crystal-field determination of Fe^{3+}. Carnegie Institution of Washington Year Book 71, 531–534.

Beran, A. (1976) Messung des Ultrarot-Pleochroismus von Mineralen. XIV. Der Pleochroismus der OH-Streckfrequenz in Diopsid. Tschermaks mineralogische und petrographische Mitteilungen, 23, 79–85.

Burns, R.G., and Strens, R.G.J. (1966) Infrared study of the hydroxyl bonds in clinoamphiboles. Science, 153, 890–892.

Carlson, W.D. (1986a) Vanadium pentoxide as a high-temperature solvent for phase equilibrium studies in CaO-MgO-Al_2O_3-SiO_2. Contributions to Mineralogy and Petrology, 92, 89–92.

——— (1986b) Reversed pyroxene phase equilibria in CaO-MgO-SiO_2 from 925° to 1,175°C at one atmosphere pressure. Contributions to Mineralogy and Petrology, 92, 218–224.

Clowe, C.A., Popp, R.K., and Fritz, S.J. (1988) Experimental investigation of the effect of oxygen fugacity on ferric-ferrous ratios and unit

cell parameters of four natural clinoamphiboles. American Mineralogist, 73, 487–499.

Deer, W.A., Howie, R.A., and Zussman, J. (1966) An introduction to the rock-forming minerals, 528 p. Longmans, Essex, England.

Dollase, W.A., and Gustafson, W.I. (1982) ^{57}Fe Mössbauer spectral analysis of the sodic clinopyroxenes. American Mineralogist, 67, 311–327.

Dyar, M.D., McGuire, A.V., and Mackwell, S.J. (1992) Fe^{3+}/H^{+} and D/H in kaersutites: Misleading indicators of mantle source fugacities. Geology, 20, 565–568.

Ghose, S., Kersten, M., Langer, K., Rossi, G., and Ungaretti, L. (1986) Crystal field spectra and Jahn Teller effect of Mn^{3+} in clinopyroxene and clinoamphiboles from India. Physics and Chemistry of Minerals, 13, 291–305.

Huebner, J.S. (1987) Use of gas mixtures at low pressure to specify oxygen and other fugacities of furnace atmospheres. In G.C. Ulmer and H.L. Barnes, Eds., Hydrothermal experimental techniques, p. 20–60. Wiley, New York.

Ingrin, J., Latrous, K., Doukhan, J.C., and Doukhan, N. (1989) Water in diopside: An electron microscopy and infrared spectroscopy study. European Journal of Mineralogy, 1, 327–341.

Mackwell, S.J., and Kohlstedt, D.L. (1990) Diffusion of hydrogen in olivine: Implications for water in the mantle. Journal of Geophysical Research, 95, 5079–5088.

Morimoto, N., Ferguson, A.K., Ginzburg, I.V., Ross, M., Seifert, F.A., Zussman, J., Aoki, K., and Gottardi, G. (1988) Nomenclature of pyroxenes. American Mineralogist, 73, 1123–1133.

Rossman, G.R., and Smyth, J.R. (1990) Hydroxyl contents of accessory minerals in mantle eclogites and related rocks. American Mineralogist, 75, 775–780.

Skogby, H., and Rossman, G.R. (1989) OH^{-} in pyroxenes: An experimental study of incorporation mechanisms and stability. American Mineralogist, 74, 1059–1069.

——— (1991) The intensity of amphibole OH bands in the infrared absorption spectrum. Physics and Chemistry of Minerals, 18, 64–68.

Skogby, H., Bell, D.R., and Rossman, G.R. (1990) Hydroxide in pyroxene: Variations in the natural environment. American Mineralogist, 75, 764–774.

Skogby, H., Annersten, H., Domeneghetti, M.C., Molin, G.M., and Tazzoli, V. (1992) Iron distribution in orthopyroxene: A comparison of Mössbauer spectroscopy and X-ray refinement results. European Journal of Mineralogy, 4, 441–452.

Smyth, J.R., Bell, D.R., and Rossman, G.R. (1991) Incorporation of hydroxyl in upper-mantle clinopyroxenes. Nature, 351, 732–735.

Smyth, J.R., Swope, R.J., and McCormick, T.C. (1992) Crystal chemistry and the role of hydrous clinopyroxenes in the mantle (abs.). Eos, 73, p. 141.

Wilkins, R.W.T., and Sabine, W. (1973) Water content of some nominally an hydrous silicates. American Mineralogist, 58, 508–516.

Manuscript received March 10, 1993
Manuscript accepted November 4, 1993